Planetary Defense Conference 2013

IAA-PDC13-04-08

Target Selection for a Hypervelocity Asteroid Intercept Vehicle Flight Validation Mission

Sam Wagner[a,1,*], Bong Wie[b,2], Brent W. Barbee[c,3]

[a]*Iowa State University, 2271 Howe Hall, Room 2348, Ames, IA 50011-2271, USA*
[b]*Iowa State University, 2271 Howe Hall, Room 2325, Ames, IA 50011-2271, USA*
[c]*NASA/GSFC, Code 595, 8800 Greenbelt Road, Greenbelt, MD, 20771, USA, 301.286.1837*

Abstract

Asteroids and comets have collided with the Earth in the past and will do so again in the future. Throughout Earth's history these collisions have played a significant role in shaping Earth's biological and geological histories. The planetary defense community has been examining a variety of options for mitigating the impact threat of asteroids and comets that approach or cross Earth's orbit, known as near-Earth objects (NEOs). This paper discusses the preliminary study results of selecting small (100-m class) NEO targets and mission design trade-offs for flight validating some key planetary defense technologies. In particular, this paper focuses on a planetary defense demo mission for validating the effectiveness of a Hypervelocity Asteroid Intercept Vehicle (HAIV) concept, currently being investigated by the Asteroid Deflection Research Center (ADRC) for a NIAC (NASA Advanced Innovative Concepts) Phase 2 project.

Introduction

Geological evidence shows that asteroids and comets have collided with the Earth in the past and will do so in the future. Such collisions have played an important role in shaping the Earth's biological and geological histories. Many researchers in the planetary defense community have examined a variety of options for mitigating the impact threat of Earth approaching or crossing asteroids and comets, known as near-Earth objects (NEOs).

As early as 1992, the idea of discovering and tracking near-Earth objects (NEOs) was proposed to the U.S. Congress [1]. That search effort, called the Spaceguard Survey, was later implemented in 1998 with the ultimate goal of finding 90% of the estimated asteroid population 1 km in diameter or larger by 2008. By focusing on only 1 km size or larger NEOs, that survey only intended to find NEOs large enough to cause global catastrophes. While not large enough to affect the entire globe, impacts by objects smaller than 1 km occur more frequently and are capable of causing significant damage. In 2005, the George E. Brown, Jr. Near-Earth Object Survey Act expanded the original Spaceguard search to include the detection and characterization of 90% of NEOs as small as 140 m by the year 2020. To date, none of the discovered objects are predicted to be on a collision course with the Earth, but the survey still has 8 more years to operate until completion. Should a new NEO be discovered on a collision course with the Earth, a mitigation effort would have to be undertaken to prevent the collision.

Given a lead time (from initial detection of the incoming NEO) of at least 10 to 20 years, depending on circumstances, various proposed technologies such as kinetic impactors, slow-pull gravity tractors, or solar sails could be employed to successfully mitigate an impact threat by deflecting the NEO's heliocentric orbit just enough to avoid a collision with Earth. When the warning time is short, however, nuclear technologies for a standoff, contact, or subsurface explosion may be the only viable options. However, as of the time of this writing none of the aforementioned mitigation options have been validated with a flight demonstration mission. The Asteroid Deflection Research Center (ADRC) has conducted a preliminary design for Hypervelocity Asteroid Intercept

*Corresponding author
Email addresses: thewags@iastate.edu (Sam Wagner), bongwie@iastate.edu (Bong Wie), brent.w.barbee@nasa.gov (Brent W. Barbee)
[1]Graduate Research Assistant, Asteroid Deflection Research Center, Department of Aerospace Engineering
[2]Aerospace Engineer, Navigation and Mission Design Branch
[3]Vance Coffman Endowed Chair Professor, Asteroid Deflection Research Center, Department of Aerospace Engineering

Vehicle (HAIV), a spacecraft capable of performing hypervelocity (> 5 km/s) intercept of asteroids as small as a 50–100 meters in diameter [2–4]. In this paper a variety of mission analysis results will be presented to illustrate candidate target asteroids for a flight validation of the HAIV spacecraft. The mission concepts considered include direct intercept missions, in which the impactor is inserted directly on an intercept course by the launch vehicle and is only allowed to perform small ΔV maneuvers prior to impact.

To measure the performance and success of the HAIV spacecraft it would be useful to have an observer spacecraft at the asteroid prior to the time at which the HAIV interceptor impacts the asteroid. However, due to mission and launch vehicle cost constraints it is highly desirable to perform the entire mission using one launch vehicle. Towards that end, we have designed the flight validation mission such that an observer spacecraft is not strictly required; instead, the HAIV transmits adequate telemetry to Earth for reconstruction of the asteroid impact event. The flight validation mission design is made even more cost-effective by incorporating advanced interplanetary mission design techniques including optimally placed deep space maneuvers (DSMs) and both powered and unpowered gravity assists via planetary flybys.

Previous and Future NEO Missions

To help determine the mission requirements and constraints it is useful to examine past and proposed future robotic missions to NEOs. Space agencies such ESA, JAXA, and NASA have had several successful missions that demonstrate technology and mission capabilities that are relevant to the proposed HAIV demonstration mission, including terminal guidance targeting and/or landing capabilities. Some of the most notable missions are the Hayabusa Mission by JAXA, and the NEAR-Shoemaker and Deep Impact missions by NASA. The Hayabusa spacecraft, formerly known as MUSES-C, was sent to the asteroid 25143 Itokawa, a near-Earth asteroid (NEA) $535 \times 294 \times 209$ m in size. While at the asteroid, the spacecraft performed two landings for the purpose of collecting surface samples, which were subsequently returned to Earth in June 2010. However, problems with the sample collection mechanism resulted in only tiny grains of asteroid material being returned. The spacecraft also had a small lander onboard, called MINERVA, that was to be guided to the surface of the asteroid. Unfortunately, the lander drifted into space and was unable to complete its mission. The NEAR-Shoemaker mission was designed to study the asteroid 433 Eros, which is one of the largest NEOs at $34.4 \times 11.2 \times 11.2$ km in size. This spacecraft was the first to orbit an asteroid as well as the first to land on one. While the Hayabusa and NEAR-Shoemaker missions were designed to softly touch down on the surface of their respective asteroids, the Deep Impact mission was designed to do just the opposite. Approximately 24 hours prior to impact with the comet Tempel 1, which is 7.6×4.9 km in size, the impactor was separated from the flyby spacecraft and autonomously navigated to ensure a hypervelocity impact at a relative speed of 10.3 km/s.

More recently, ESA proposed a demonstration mission for a kinetic-impactor called the Don Quijote mission [5, 6]. The mission concept called for two separate spacecraft to be launched at the same time but follow different interplanetary trajectories. Sancho, the orbiter spacecraft, would be the first to depart Earth's orbit, and rendezvous with a target asteroid approximately 500 m in diameter. Sancho would measure the position, shape, and other relevant characteristics before and after a hypervelocity impact by Hidalgo, the impactor spacecraft. After Sancho studied the target for some months, Hidalgo would approach the target at a relative speed of approximately 10 km/s. Sancho then observes any changes in the asteroid and its heliocentric orbit after the kinetic impact to assess the effectiveness of this deflection strategy. Don Quijote was planned to launch in early 2011 and complete its mission in mid to late 2017. However, the mission concept was never realized due to higher than expected mission costs.

Table 1: Target Selection Criteria for the Don Quijote Mission.

Orbit Characteristics	Preferred Range
Rendezvous ΔV	< 7 km/s
Orbit type	Amor
MOID	large and increasing
Orbit accuracy	well determined orbits
Physical Characteristics	**Preferred Range**
Size	< 800 m
Density	~1.3 g/cm^3
Absolute magnitude	20.4 - 19.6
Shape	not irregular
Taxonomic type	C-type
Rotation period	< 20 hours
Binarity	not binary

The selection process for the Don Quijote mission was based on a set of NEO characteristics defined by ESA's NEOMAP in Table 1 [7, 8]. Their analysis resulted in the selection of the asteroids 2002 AT4 and 1989 ML. As seen in Table 2, 2002 AT4 is roughly half the size of 1989 ML, but intercepting it requires more ΔV. A realistic deflector spacecraft would require a versatile design capable of intercepting and deflecting or disrupting either target on short notice.

Table 2: Properties of Candidate Targets Considered for the Don Quijote Mission.

	2002 AT4	1989 ML
Orbital period (yr)	2.549	1.463
e	0.447	0.137
i	1.5°	4.4°
ΔV (km/s)	6.58	4.46
Orbit type	Amor	Amor
MOID	large	large
Absolute magnitude	20.96	19.35
Taxonomic type	D-type	E-type
Diameter (m)	380	800
Rotational period (hr)	6	19

One last notable future mission planned by NASA is the OSIRIS-REx asteroid sample return mission, which will return a sample from NEA 101955 (1999 RQ36). This mission will launch in September of 2016 and will return the sample to Earth in September of 2023. This mission will utilize large DSMs, Earth gravity assist (GA), rendezvous and proximity maneuvers, and an asteroid departure maneuver. The proposed HAIV demonstration mission will incorporate a combination of the knowledge gained from the development and execution of these NEO science missions.

Near-Earth Asteroid (NEA) Groups

For the purposes of this study, NEAs in the Atira and Amor orbit groups were considered. A comparison of NEA orbit families is shown in Figure 1. NEAs in these groups all have perihelion distances < 1.3 AU, and many of them also cross the Earth's orbit at some point. The proximity of NEA orbits to Earth's orbit means that the ΔV required for intercept is usually small. As such, we expect that a number of NEAs will prove to be viable candidates for an NEA deflection/disruption flight validation mission. Apollo and Aten NEA orbits cross Earth's orbit, and in some cases this leads to lower mission ΔV requirements as compared to Atiras or Amors. On the other hand, this same fact means that any significant perturbation to the NEA's orbit could cause it to later impact the Earth. While unlikely, we do not want our demonstration of deflection technologies to cause such a thing to happen. The ESA also had this in mind when they selected the asteroids 2002 AT4 and 1989 ML from the Amor group for the Don Quijote mission concept [5].

To preclude the possibility of inadvertently perturbing a previously harmless NEA onto an Earth collision course, we consider only Atira and Amor NEAs in our study. The Amor asteroid group is characterized by asteroids that approach the Earth, but do not actually cross its orbit. By definition the perihelion distances of these asteroids lie between 1.017 and 1.3 AU. As of July 21st, 2012, there were 3398 Amor and Atira asteroids listed in NASA's NEO Program database[4]. While Amor asteroids are entirely outside of the Earth's orbit, the Atira asteroid group orbits are contained entirely within the orbit of the Earth. Because the orbits of Atiras and Amors are entirely interior or exterior to Earth's orbit, respectively, disturbances to the orbits of those asteroids are not likely to cause an impact with the Earth at any time after the mission.

Mission Design Software

In addition to the HAIV concept design the ADRC has also developed mission design software tools capable of performing advanced mission analysis for thousands of potential target asteroids. Due to the large of variables in these types of missions, an exhaustive search of all 3398 asteroids would be impractical. In addition, all mission design computation will be performed using an evolutionary algorithm known as a genetic algorithm. The types of missions considered in this paper can easily be formulated as constrained optimization problems, making them ideal for evolutionary algorithms. For this approach, each mission type must first be formulated as a single-valued cost function.

[4] `http://neo.jpl.nasa.gov/stats/`

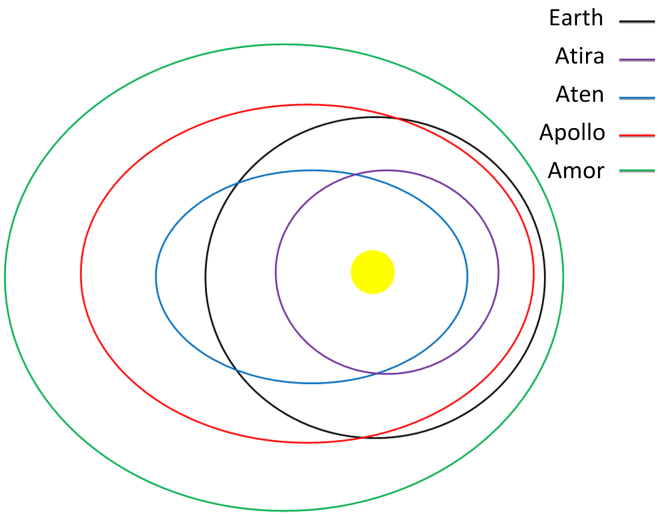

Figure 1: Comparison of Atira, Apollo, Aten, and Amor class asteroid orbits in relation to the Earth's orbit.

Utilizing a combination of evolutionary algorithms, modular mission design software, and modern Graphics Processing Units (GPUs) allows multiple possible mission architectures for thousands of possible target asteroids to be quickly and efficiently analyzed. Given the capabilities of the mission design software several types of missions have been considered and are detailed in the following section. Details of the genetic algorithm are presented in Appendix A.

Problem Formulation and Mission Constraints

The purpose of this paper is to determine realistic mission designs for a HAIV demonstration that can be flown in the near future. Several mission constraints are imposed during the mission design searches to ensure that the resulting missions are realistic at the level of the current analysis. These constraints are enforced via penalty functions that shape the solutions and ensure the best optimal solutions are found while respecting constraints.

The first constraint imposed ensures that the HAIV spacecraft will be able to communicate with Earth ground stations during the final impact phase of the mission. This is done by penalizing any missions where the impact would occur on the opposite side of the sun from the Earth. The exact angle limitations for the impact Earth-Asteroid angle are that the angle must be < 175 degrees from the Earth and > 185 degrees from the Earth. Figure 2 illustrates the line of sight angular constraints. The second main constraint is a guidance and navigation constraint such that the impactor approaches from the sunward side of the asteroid. This constraint ensures proper lighting conditions for the terminal guidance phase of the mission.

The purpose of this mission is to demonstrate the feasibility of the HAIV spacecraft for the purpose of planetary defense. The HAIV spacecraft is designed for the sort of hypervelocity impacts that are likely to be required by planetary defense missions executed with short warning time. Therefore, missions designed in this paper must have a minimum impact velocity of 5 km/s. Due to anticipated technological limitations, impact velocities over 30 km/s are penalized as well. However, it should be noted that none of the mission analyzed have had an impact velocity above 30 km/s, meaning the HAIV impactor never has to propulsively decrease its approach velocity. All other major mission constraints can be found in Table 3. The exact penalty functions are also discussed at the end of this section. It is worth noting that limitations on NEA orbit group and absolute magnitude (H) reduce the number of asteroids that much be searched from approximately 3500 to 1500.

Depending on mission complexity, there are different ways to formulate multiple gravity-assist problems (simple direct intercept missions are a subset of the MGA model). Simple missions, such as NASA's Voyager, Pioneer, and Galileo missions, which don't require large DSMs, can be formulated using the MGA model. This model requires fewer variables than the MGA-DSM model, meaning they have a much lower computational cost. On many occasions, small DSMs, when compared to the departure and arrival maneuvers, can significantly lower the total overall mission cost in terms of minimizing total ΔV or maximizing arrival mass. The formulation for both types of missions are included in the following subsections. Most of the solution algorithms needed for both problem types will be included. However, expositions of solutions to Lambert's problem, solutions to Kepler's equation, date conversion algorithms, and so on are omitted for brevity.

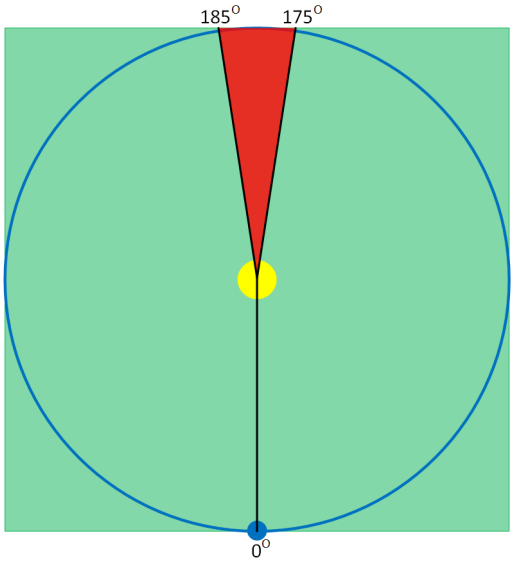

Figure 2: Illustration of the Earth-Sun-Asteroid line-of-site communication angle for the HAIV mission. Green indicates communicable from Earth ground stations, while red indicates area where communications are not possible..

Table 3: List of mission constraints.

Asteroid Types	Amor, Atira
Earlier Launch Date	1-Jan-18
Latest Launch Date	31-Dec-22
Minimum Impact Velocity	5 km/s
Maximum Impact Velocity	30 km/s
H Magnitude Range	20.75-23.62
Communication LOS Constraints	> 185 and < 175 deg
Impact Angle Constraint	Penalized if approach isn't from the sunward side
Impactor Limitations	For dual missions the impact must occur after rendezvous s/c arrival
Maximum Departure C_3	12.5 km^2/s^2 for single s/c mission, 30 km^2/s^2 for dual s/c missions

The intent of both methods is to determine a final cost function that the genetic algorithm can optimize. That is, minimize or maximize, depending on how the individual problem is formulated. Cost functions typically consist of all of the required mission ΔVs, the Earth departure V_∞, the final arrival V_∞, and any other mission constraints. Any permutation of these elements can be used for each specific mission type analyzed in this paper. For instance in this study the departure C_3 only affects the final cost function if it is above 12.5 km^2/s^2 for the single spacecraft missions and 30 km^2/s^2 for the dual spacecraft missions. In space mission design this is often done because the launch vehicle upper stage can be leveraged for the Earth departure maneuver (typically, limited by C_3). It is worth noting that for the genetic algorithm used in this paper, all mission constraints are applied directly in the cost function.

Multiple Gravity-Assist Model

For the multiple gravity-assist model, two Lambert solutions are essentially "patched" together using the standard patched conics method. This results in a powered hyperbolic trajectory for each gravity assist in which a ΔV is allowed only at the periapsis passage of each gravity assist. The ΔV at each gravity assist is part of the final cost function, and is usually driven to a near-zero value.

For each gravity assist, the incoming and outgoing velocity vectors (in the heliocentric frame) are provided by Lambert's problem solutions. The velocities relative to the planets are then found as:

$$\vec{v}_{\infty-in} = \vec{V}_{s/c-in} - \vec{V}_{\oplus} \tag{1}$$

$$\vec{v}_{\infty-out} = \vec{V}_{s/c-out} - \vec{V}_{\oplus} \tag{2}$$

From this point the goal is to determine a method to find the periapsis radius that is required to patch the two solutions together. The first step is to determine the semi-major axis of the incoming and outgoing hyperbolic trajectories.

$$a_{in} = -\frac{\mu_{\oplus}}{v_{\infty-in}^2} \tag{3}$$

$$a_{out} = -\frac{\mu_{\oplus}}{v_{\infty-out}^2} \tag{4}$$

where $\mu_{\oplus}$ is the target planet's gravitational parameter.

The required turning angle is:

$$\delta = \cos^{-1}\left(\frac{\vec{v}_{\infty-in} \cdot \vec{v}_{\infty-out}}{v_{\infty-in} \cdot v_{\infty-out}}\right) \tag{5}$$

The flyby periapsis radius is equal for both legs of the hyperbolic orbit. That is, we have

$$r_p = a_{in}(1 - e_{in}) = a_{out}(1 - e_{out}) \tag{6}$$

where e_{in} and e_{out} are the incoming and outgoing orbit eccentricities. It should be noted that the orbits will be hyperbolic, so both eccentricities will be greater than 1. The turning angle δ can also be represented as the sum of the transfer angles for the incoming and outgoing orbits.

$$\delta = \sin^{-1}\left(\frac{1}{e_{in}}\right) + \sin^{-1}\left(\frac{1}{e_{out}}\right) \tag{7}$$

Equation 6 can be solved for e_{in}, as

$$e_{in} = \frac{a_{out}}{a_{in}}(e_{out} - 1) + 1 \tag{8}$$

Substituting Eq. 8 into Eq. 7 gives

$$\delta = \sin^{-1}\left(\frac{1}{\frac{a_{out}}{a_{in}}(e_{out} - 1) + 1}\right) + \sin^{-1}\left(\frac{1}{e_{out}}\right) \tag{9}$$

which can be rewritten as

$$f = \left(\frac{a_{out}}{a_{in}}(e_{out} - 1)\right)\sin\left(\delta - \sin^{-1}\left(\frac{1}{e_{out}}\right)\right) - 1 = 0 \tag{10}$$

The above equation, which is now only a function of e_{out}, can be iterated upon to solve for e_{out}. A simple Newton iteration scheme works well. For this the derivative of f with respect to e_{out} must first be found.

$$\frac{df}{de_{out}} = \left(\frac{a_{out}}{a_{in}}e_{out} - \frac{a_{out}}{a_{in}} + 1\right)\frac{\cos\left(\delta - sin^{-1}\frac{1}{e_{out}}\right)}{e_{out}^2\sqrt{1 - \frac{1}{e_{out}^2}}} + \frac{a_{out}}{a_{in}}\sin\left(\delta - \sin^{-1}\frac{1}{e_{out}}\right) \tag{11}$$

To start the Newton iteration, an initial value for e_{out} of 1.5 works well. In a typical Newton iteration scheme, a `do-while`loop is used until e_{out} stops changing within a certain tolerance. The iteration number inside the loop should also be monitored so that the loop can be exited if convergence doesn't occur. Each new e_{out} is calculated as:

$$e_{new} = e_{old} - \frac{f}{\frac{df}{de_{out}}} \tag{12}$$

When converged, e_{out} is known and the periapsis radius is calculated from Eq. 6. Finally, the ΔV that must be applied at periapsis is determined as

$$\Delta V_{GA} = \left|\sqrt{v_{\infty-in}^2 + \frac{2\mu_{\oplus}}{r_p}} - \sqrt{v_{\infty-out}^2 + \frac{2\mu_{\oplus}}{r_p}}\right| \tag{13}$$

The flyby periapsis radius and ΔV are determined directly from the spacecraft's incoming and outgoing velocities. These are provided by solutions to Lambert's problem, which are a function of planetary positions and times of flight. The planetary positions are also a function of time, meaning that the decision variables for the

MGA model are the time of Earth departure, time of each gravity assist, and final arrival time. Thus the final cost function C for the MGA optimization problem is represented as

$$C = f(\mathbf{X}) + g(\mathbf{X}) \tag{14}$$

$$\mathbf{X} = [T_0, T_1 \dots T_f]^T \tag{15}$$

In this case T_0 is the launch date, T_i is the time of flight for each leg of the mission, and T_f is time of flight for the final mission leg. The penalty function, $g(\mathbf{X})$ will be covered later. As shown above each element of the cost function, ΔVs, etc, are only a function of time. This MGA cost function can then be optimized by the genetic algorithm to find optimal or near optimal solutions.

Multiple Gravity-Assist Deep Space Maneuver Model

The MGA model, while simple and easy to implement, is not suitable for all missions. It is often the case that allowing DSMs, where the ΔV is applied sometime during the interplanetary coast arc rather than at the flyby periapsis, yields a more optimal solution. This simply implies that the optimal location for mission maneuvers may not be at the flyby periapses. It was for this reason that the MGA-DSM model was originally developed. This section will outline the basics necessary to implement this model and is based on Ref. [9–13].

In the MGA-DSM model the mission is broken down into three phases, Earth departure, gravity assist, and the final terminal phase. For the Earth departure phase an impulsive ΔV can be applied in any direction from Earth. This can be defined by three variables, the v_∞ magnitude (or, equivalently, C_3), and the departure right ascension and declination angles, α and β, respectively. Three additional variables are also needed to completely describe the model, namely the launch date, time of flight from launch to the first flyby, and the burn index (ϵ). The burn index is used to define the point along the trajectory in which a ΔV will be applied to target the next planet in the sequence. The burn index varies between 0 and 1, although both 0 and 1 would represent a simple Lambert solution without any additional maneuvers. Constraining the range of allowable departure declinations has the added benefit of ensuring that any trajectories found will be compatible with the published performance parameters for a given launch vehicle (in terms of mass delivered to particular C_3). Launch vehicles often have reduced performance when the departure declination is outside the stated range of values, but the details are rarely provided in published launch vehicle user guides. The spacecraft's initial state vector at Earth departure is:

$$\vec{r}_{s/c} = \vec{r}_\oplus(T_0) \tag{16}$$

$$\mathbf{V}_{s/c} = \mathbf{V}_\oplus(T_{launch}) + v_\infty \begin{bmatrix} \cos\alpha\cos\beta \\ \sin\alpha\cos\beta \\ \sin\beta \end{bmatrix} \tag{17}$$

From this point on, the next step is the essentially same for both the departure phase and gravity assist phases. The spacecraft's state vector is propagated forward by a time $\epsilon_1 T_1$, at which point a DSM is applied to target the next planet. This targeting is performed by applying a solution to Lambert's problem, with the time of flight given by $(1-\epsilon_1)T_1$. The magnitude of the DSM is just the magnitude of the difference between the velocity vector after the orbit is propagated and the initial velocity vector from the Lambert's solution. The planetary arrival velocity, also from the Lambert solver, is then used for the next phase of the mission.

An additional four variables are necessary for each gravity assist phase of the trajectory: the flyby radius ratio (r_{pi}), b-plane insertion angle (γ_i), time of flight (T_i), and burn index (ϵ_i). In this case i is the gravity assist number of the trajectory. The periapsis radius ratio directly defines the periapsis radius. In this formulation the periapsis radius is a variable, rather than being defined by the problem geometry. In order for the incoming and outgoing hyperbolas to be defined, the incoming and outgoing v_∞ magnitudes are set equal.

$$R_{pi} = r_{pi} R_\oplus \tag{18}$$

$$\left|\vec{v}_{\infty-in}\right| = \left|\vec{v}_{\infty-out}\right| \tag{19}$$

Similar to the the MGA model, the incoming velocity vector is given by

$$\vec{v}_{\infty-in} = \vec{V}_{s/c-in} - \vec{V}_\oplus \tag{20}$$

The eccentricity must be found from the patched conic model [14]. In the MGA-DSM model the arrival and departure v_∞ magnitudes are defined to be the same, thus the semi-major axis and eccentricity are the same for both arrival and departure trajectories described by

$$a = -\frac{\mu_\oplus}{v_\infty^2} \tag{21}$$

$$e = 1 - \frac{R_{pi}}{a} \tag{22}$$

The flyby turning angle is given by

$$\delta = 2 \arcsin \frac{1}{e} \tag{23}$$

The outgoing v_∞ is the obtained from the following four equations:

$$\vec{v}_{\infty-out} = v_\infty \left[\cos\delta\hat{i} + \cos\gamma_i \sin\delta\hat{j} + \sin\gamma_i \sin\delta\hat{k}\right] \tag{24}$$

$$\hat{i} = \frac{\vec{v}_{\infty-in}}{\left|\vec{v}_{\infty-in}\right|} \tag{25}$$

$$\hat{j} = \frac{\hat{i} \times \vec{V}_{\infty-in}}{\left|\hat{i} \times \vec{V}_{\infty-in}\right|} \tag{26}$$

$$\hat{k} = \hat{k} \times \hat{j} \tag{27}$$

The outgoing velocity is found in the same way as it is in the MGA model, as follows:

$$\vec{V}_{s/c-out} = \vec{v}_{\infty-out} + \vec{V}_\oplus \tag{28}$$

Similar to the Earth departure phase, the spacecraft is propagated forward by $\epsilon_i T_i$ time. Then the next planet is targeted using a Lambert solver. The DSM is found as it is in the departure phase of the trajectory.

The terminal phase of the mission can be formulated in multiple ways. The DSM which targets the final planet is part of the prior flyby cost function, so the only addition to the cost function is typically either the arrival v_∞ or a ΔV for a specific orbit insertion. Often the orbit about the final planet is defined by an insertion periapsis radius and insertion eccentricity or orbit period.

The cost function is represented in the same way as the MGA model. However, the number of total state variables is increased significantly when compared to the MGA model. As before, $f(\mathbf{X})$ is the actual cost function (mission ΔVs, etc) and $g(\mathbf{X})$ is a penalty function used to enforce and problem constraints. n is defined to be the number of gravity assist required by the mission.

$$C = f(\mathbf{X}) + g(\mathbf{X}) \tag{29}$$

$$\mathbf{X} = [T_0, v_{\infty-0}, \alpha_0, \beta_0, \epsilon_0, T_l, T_1 \ldots T_{n+1}, \epsilon_1 \ldots \epsilon_n, \gamma_1 \ldots \gamma_n, r_{p1} \ldots r_{pn}]^T \tag{30}$$

In Eq. 30, n is the number of gravity-assists to be performed. An example final form of a typical cost function, without any constraint penalties, is expressed as

$$C = v_{\infty-0} + \Delta V_0 + \Delta V_1 \ldots \Delta V_n + v_{\infty-f} \tag{31}$$

where ΔV_i is the magnitude of the DSM corresponding to an accompanying planetary flyby.

Problem Constraints

In optimization problems, constraints are often used to help shape the final solution. When implementing genetic algorithms, constraints are used, rather than hard limits, in order to keep to solution space open. If the solution space isn't sufficiently large the genetic algorithm will be unable to start, due to the random initialization process.

Common constraints for mission design problems include periapsis radius during a gravity assist, mission time/leg length constraints, and guarding against low velocity flybys. During a low-velocity flyby the spacecraft is captured by the planet instead of gaining velocity in the heliocentric frame. Any other constraint the user wishes impose to help shape the solution can be added, as long as the constraint values are approximately the same order of magnitude at the actual cost function values. It should be noted that when using the MGA-DSM model in conjunction with a genetic algorithm all of the variables can be explicitly constrained. However, low-velocity flybys can still occur. Specific HAIV mission constraints imposed include maximum C_3, Earth-Sun

communication angles, final terminal approach angles, impactor approach velocity, and a time constraint that ensures the rendezvous spacecraft arrives prior to hypervelocity impactor.

It is often the case the MGA model results in a periapsis radius that is less than the planet's physical radius or is too close to the planet's atmosphere. In this situation a constraint-handling method is necessary to move the solution toward more feasible solutions. The method below is from Englander, et al [10].

$$g_i(\mathbf{X}) = -2\log\frac{R_{pi}}{kR_{\oplus}} \tag{32}$$

where k is a multiplier used to define how close the spacecraft is allowed to fly by a target planet. For all of the examples in this paper a value of 1.1 was used.

The second constraint penalty method penalizes low-velocity flybys. The method has also been adapted from Englander et a.l [10] Low-velocity flybys are very rare, but solutions should still be protected from converging on them. The orbital energy relative to the flyby planet can be calculated as

$$E = \frac{\left|\vec{v}_{\infty-in}\right|^2}{2} - \frac{\mu_{\oplus}}{R_{soi}} \tag{33}$$

For the flyby trajectory to be hyperbolic relative to the planet, E must be greater than zero. However, the sphere of influence model is an approximation, so an additional 10% margin on the incoming velocity needs to be added. For relatively large v_∞ the penalty is zero or very small compared to the overall cost function value. Alternatively, for very low v_∞ values the penalty is large enough to severely influence the final shape of the solution. The flyby orbital energy, adjusted for the 10% margin, and final constraint are calculated using the following two equations:

$$E = \frac{\left|0.9\vec{v}_{\infty-in}\right|^2}{2} - \frac{\mu_{\oplus}}{R_{soi}} \tag{34}$$

$$g_i(\mathbf{X}) = \begin{cases} 0 & E \geq 0 \\ \frac{1}{\left|\vec{v}_{\infty-in}\right|} & E < 0 \end{cases} \tag{35}$$

For the MGA model, trajectories can be found with Earth departure C_3 values that exceed the specified limit. The penalty function is formulated to represent that additional Earth departure ΔV beyond that provided by the launch vehicle's upper stage would be required from the HAIV spacecraft in order to attain the required C_3. The exact penalty function is

$$g_i(\mathbf{X}) = \begin{cases} v_{\infty-l} - \sqrt{C_{3max}} & v_{\infty-l} > \sqrt{C_{3max}} \\ 0 & v_{\infty-l} \leq \sqrt{C_{3max}} \end{cases} \tag{36}$$

The following time constraint is used to ensure that the rendezvous spacecraft arrives at the asteroid prior to the arrival of the HAIV spacecraft.

$$g_i(\mathbf{X}) = \begin{cases} 0.1(T_{rend.-arrival} - T_{impactor-arrival}) & T_{rend.-arrival} > T_{impactor-arrival} \\ 0 & T_{rend.-arrival} \leq T_{impactor-arrival} \end{cases} \tag{37}$$

The next constraint is added to ensure the communication line-of-site angle is feasible during the final terminal impact phase. This is especially important in the absence of an observer spacecraft, as communications with the Earth just prior to impact will be the only way to determine mission success. $\vec{R}_{\oplus}$ is the Earth radius vector at impact, while $\vec{R}_{ast}$ is the asteroid radius vector at impact. The line-of-site angle is then found as

$$LOS = \cos^{-1}\left(\frac{\vec{R}_{\oplus}\cdot\vec{R}_{ast}}{R_{\oplus}R_{ast}}\right) \tag{38}$$

To ensure the LOS angle is in the right quadrant, the z component of the cross product of the two radius vectors is utilized as follows

$$\vec{c} = \vec{R}_{\oplus}\times\vec{R}_{ast} \tag{39}$$

$$LOS = 2\pi - LOS \quad c(3) \leq 0 \tag{40}$$

The final penalty function for the LOS angle constraints is given in the following constraint equation:

$$g_i(\mathbf{X}) = \begin{cases} \exp\left(\frac{-1}{1-(LOS-180)^2}\right) & 175^\circ \leq LOS \leq 185^\circ \\ 0 & for\ all\ other\ angles \end{cases} \tag{41}$$

The final penalty function used to ensure mission feasibility penalizes the relative asteroid velocity with respect to the asteroid's position relative to the sun. This ensures that the spacecraft arrives on the sunward side of the asteroid, which results in lighting conditions that are favorable for the terminal guidance system. The asteroid radius and impactor relative velocity unit vectors are utilized to preclude numerical scaling issues. Unlike the time and LOS angle penalties, all angles greater than 0 (which corresponds to approaching directly along the asteroid-sun line from the sunward side) are penalized with a linear function. This is done because the approach angle is one of the most critical parameters to ensure mission success.

$$SA = \cos^{-1}(\vec{e}_r \cdot \vec{e}_v) \tag{42}$$

$$g_i(\mathbf{X}) = \frac{1}{\pi} SA \tag{43}$$

Additional penalty constraint functions can be added to shape the solution as the user desires. The final constraint function is the sum of the individual constraint functions given by

$$g(\mathbf{X}) = \sum g_i(\mathbf{X}) \tag{44}$$

With the cost function for each method finalized then next step is to develop the genetic algorithm capable of optimizing these types of advanced mission design problems.

Mission Analysis Results

In this section the mission design results for the various mission architectures considered in the study are presented. Each of these mission types can be constructed using the methods described in the previous section. The genetic algorithm described in Appendix A was then used to optimize each constructed cost function using the mission constraints. More details on common limits used for each variable can be found in [10, 12, 13]. For each mission type approximately 1500 potential target asteroids were scanned for feasible missions. The results presented in the following three subsections are subsets of the standard MGA model, while all other results are subsets of the MGA-DSM model.

Direct Intercept Missions

For the direct intercept mission the launch vehicle is used to inject the HAIV spacecraft into an interplanetary orbit that directly intercepts the target asteroid. This is the simplest mission type analyzed, with only two variables to optimize (launch date and time-of-flight to the asteroid), and yields the largest number of feasible target asteroids. For direct intercept missions a relatively low C_3 limit of 12.5 km^2/s^2 is used. By limiting missions to low C_3s it may be possible to use a less capable (and therefore less expensive) launch vehicle than for missions that include both an impactor and rendezvous (observer) spacecraft.

With the low C_3 limit, hundreds of potential target asteroids were found during the search. These asteroid require no ΔV from the HAIV impactor, other than small statistical course corrections during the terminal impact phase of the mission. The results presented in Table 4 represent the top 3 asteroids determined by a joint study with the Mission Design Lab (MDL) at the Goddard Spaceflight Center and the ADRC. These asteroids were chosen because their orbits are fairly well known (or future observations of them will be possible prior to the mission launch dates), the estimated diameters[5] are close to the desired diameter of 100 meters, they have low sun approach angles, and the impactor arrival velocities are high enough to be technically challenging yet feasible. How well the asteroid orbits are known is expressed by the Orbit Condition Code (OCC)[6] for the orbit, which is an integer scale ranging from 0 (a very well known orbit) to 9 (a very poorly known orbit).

[5]We estimate the asteroid diameters based on their absolute magnitude (H) values and an assumed geometric albedo of 0.25. The relationship between diameter, H, and geometric albedo is documented at `http://www.physics.sfasu.edu/astro/asteroids/sizemagnitude.html`.

[6]The OCC is also the Minor Planet Center (MPC) "U" parameter, documented at `http://www.minorplanetcenter.net/iau/info/UValue.html`.

Table 4: Top 3 asteroids for the single direct intercept mission.

Asteroid	2006 CL9	2009 QO5	2004 BW18
a (AU)	1.35	1.59	1.37
e	0.24	0.24	0.25
Diameter (m)	104.85	105.82	97.40
Departure C_3 (km^2/s^2)	11.99	12.50	12.49
Require S/C ΔV (km/s)	0.00	0.00	0.00
LOS Angle	349.01°	349.33°	333.17°
Sun Approach Angle	3.04°	28.05°	34.21°
Departure Date	2-Aug-19	27-Mar-19	7-Apr-19
TOF (days)	121.41	124.38	268.45
OCC	5	1	5
Arrival Velocity km/s	11.53	9.22	6.57

Combined Rendezvous and Direct Intercept Missions

Direct intercept missions are the baseline reference missions for the HAIV studies at the ADRC, however it may be useful to have a spacecraft at the asteroid prior to impact. This rendezvous spacecraft would likely be a small spacecraft attached to the HAIV spacecraft that would separate at some point during the mission. The goal of the following sections is to determine a trajectory solution such that the HAIV spacecraft has a relative intercept velocity greater than 5 km/s and the observer spacecraft can rendezvous with the asteroid prior to impact. Several mission types are presented that attempt to minimize the total ΔV required by both the HAIV impactor and the rendezvous spacecraft such that the mission design can be flown using existing launch vehicles.

During initial mission analysis we determined that no feasible trajectories could be found with the relatively low C_3 used for the direct intercept mission. We therefore revised the maximum allowable C_3 to 30 km^2/s^2 and considered Delta IV and Atlas V launch vehicles.

The first mission type that we analyzed employs a single DSM after the separation of the two spacecraft. For this type of mission, referred to herein as a Type 1 mission, the rendezvous spacecraft continues on a direct intercept course, while the HAIV impactor uses a DSM to target asteroid intercept at a later date. The results for Type 1 missions are shown in Table 5. The lowest total ΔV required is 3.299 km/s for asteroid 2010 KU7. However, this ΔV is likely too high to be feasible. By examining the results it appears that the impact velocity was often driven to the lower limit of 5 km/s, which indicates that lowering the minimum required impact velocity may lower the total mission ΔV.

Table 5: Top 5 asteroids by total required ΔV for Type 1 missions.

Asteroid	2010 KU7	2012 JX11	2001 CK42	2009 CR4	2000 RD53
a (AU)	1.67	1.97	1.42	1.75	1.79
e	0.381	0.475	0.281	0.419	0.428
Diameter (m)	94.74	58.42	265.80	122.62	279.61
Total ΔV (km/s)	3.299	3.518	3.711	3.737	3.755
Launch Date	3-Apr-18	3-Apr-18	3-Apr-18	3-Apr-18	3-Apr-18
Impactor TOF (days)	668.356	801.317	542.820	676.738	651.854
Rend. TOF (days)	381.743	472.330	329.512	405.902	365.241
C_3 (km^2/s^2)	25.584	33.860	16.815	33.803	24.088
Impactor DSM (km/s)	2.387	1.990	3.258	2.153	2.030
Rendezvous Arrival ΔV (km/s)	0.912	1.186	0.453	1.247	1.725
LOS	26.164°	257.769°	128.765°	19.857°	39.917°
Sun Angle	97.820°	102.315°	92.953°	94.386°	106.090°
Impactor Velocity (km/s)	5.001	5.001	5.000	5.000	5.000

The second type of mission analyzed, referred to herein as Type 2, is similar to the Type 1 mission except that the rendezvous spacecraft performs the DSM to target the asteroid at a different date than the HAIV interceptor. The top 5 results for this search are shown in Table 6. Examination of the results reveals that, on average, the total required ΔV is reduced by approximately 1 km/s, with the lowest required ΔV being approximately 2.6 km/s. Like the Type 1 mission results the impact arrival velocity is often driven to 5 km/s. As mentioned previously, reducing the minimum allowable impact velocity may reduce the total mission ΔV required.

Table 6: Top 5 asteroids by total required ΔV for type 2 missions.

Asteroid	2000 WO148	2009 TV4	1998 UM1	1996 FO3	2008 XB
a (AU)	1.64	1.69	1.7	1.44	1.51
e	0.376	0.37	0.402	0.29	0.313
Diameter (m)	198.9	59.2	60.1	212.1	81.4
Total ΔV	2.603	2.657	2.709	2.926	2.942
Launch Date	19-Jan-20	27-Sep-20	20-Sep-18	11-Feb-22	2-Dec-21
Rend TOF (days)	515.347	335.871	404.795	353.638	395.915
Impactor TOF (days)	373.451	550.537	488.660	362.521	404.855
C_3 (km^2/s^2)	26.636	29.154	33.104	16.800	24.198
Rendezvous DSM (km/s)	1.265	0.562	1.448	0.951	1.632
Rendezvous ArrivalΔV (km/s)	1.338	2.095	0.976	1.975	1.310
LOS	64.029°	198.157°	149.624°	202.840°	163.150°
Sun Angle	91.704°	100.956°	60.920°	90.103°	100.676°
Impact Velocity (km/s)	5.047	5.000	5.000	5.004	5.000

Gravity Assist(s) Missions using the MGA Model

Planetary gravity assists are often used to reduce the required ΔV for outer planet missions, and this is also possible for the missions considered herein. Gravity assist(s) can lower the average required total mission ΔV to the 1-1.5 km/s range, with some solutions found that require as little as approximately 600 m/s. For the following Type 3 and Type 4 missions the optimizer was used to decide which planet(s) should be used for the gravity assist(s). In all of the best cases presented, the Earth was found to be the best planet for the gravity assist(s). Given that most of the target asteroids have a semi-major axis between 1 and 1.3 AU, this is an intuitively satisfying result.

Type 3 missions use a single gravity assist achieved by having the HAIV impactor perform a DSM to target the planetary flyby. The gravity assist is then used to increase the velocity of the impactor, thus lowering the required ΔV when compared to Type 1 and Type 2 missions. Missions where the rendezvous spacecraft performs a gravity assist to lower the arrival ΔV were also considered, however this did not improve the total required ΔV compared to Type 1 and Type 2 missions.

A summary of the best Type 3 mission results is shown in Table 7. The best mission requires a total ΔV of approximately 1.15 km/s, which represents a nearly 1.5 km/s reduction from the best solution found for the previous mission types.

Table 7: Top 5 asteroids by total required ΔV for Type 3 missions.

Asteroid	2012 OO	2008 XB	2000 WO148	2009 CO5	1996 FO3
a (AU)	1.7	1.51	1.64	1.66	1.44
e	0.383	0.313	0.376	0.345	0.29
Diameter (m)	214.07	81.39	198.86	119.83	212.11
Total ΔV (km/s)	1.145	1.322	1.410	1.430	1.539
Launch Date	3-Sep-21	13-Dec-21	15-Jan-20	14-Mar-22	21-Feb-22
Rendezvous TOF (days)	627.812	231.753	569.599	553.895	245.288
Impactor TOF Leg 1 (days)	625.840	685.350	626.402	630.144	699.471
Impactor TOF Leg 2 (days)	70.945	226.789	156.689	716.637	275.928
C_3 (km^2/s^2)	34.509	29.678	27.570	30.354	30.460
Impactor ΔV (km/s)	0.546	0.764	0.264	0.496	1.094
Rendezvous Arrival ΔV (km/s)	0.599	0.558	1.146	0.934	0.445
Gravity Assist Planet	Earth	Earth	Earth	Earth	Earth
GA Perigee Rad (km)	7397.560	17249.044	8032.784	30908.181	13097.549
LOS	348.472°	289.519°	316.493°	332.860°	281.732°
Sun Angle	134.721°	6.243°	156.973°	164.746°	4.909°
Impactor Arrival Velocity (km/s)	5.798	5.118	6.149	5.016	5.601

The last mission type, Type 4, considered for the MGA model employs two gravity assists. The HAIV impactor targets the first gravity assist planet with a DSM. After the first gravity assist the spacecraft flies on a ballistic trajectory until the second gravity assist. This resulted in total mission ΔV being reduced from the Type 3 solutions. As was the case with Type 3 missions, the optimal gravity assist planet is the Earth for both assists. Type 4 mission

results are shown in Table 8. For these missions the lowest required total ΔV is reduced to approximately 600 m/s, ranging up to 1.3 km/s for the top 5 asteroids.

Table 8: Top 5 asteroids by total required ΔV for type 4 missions.

Asteroid	2012 CR	2011 FR17	2010 XB73	2010 GZ33	2011 AL24
a (AU)	1.77	1.7	1.71	1.91	1.72
e	0.381	0.295	0.308	0.423	0.345
Diameter (m)	120.38	55.53	102.46	90.90	91.32
Total ΔV (km/s)	0.608	1.005	1.218	1.254	1.306
Launch Date	25-Feb-19	10-Mar-22	30-Nov-19	3-Apr-18	10-Jan-20
Rendezvous TOF (days)	366.722	405.961	351.305	325.152	391.061
Impactor TOF Leg 1 (days)	692.292	702.523	694.408	682.899	692.473
Impactor TOF Leg 2 (days)	44.823	569.094	351.721	1223.708	1126.003
Impactor TOF Leg 3 (days)	605.125	533.076	540.387	767.832	565.256
C_3 (km^2/s^2)	26.788	29.499	30.623	30.008	32.096
Impactor S/C ΔV (km/s)	0.461	0.303	0.230	1.150	0.373
Rendezvous Arrival ΔV (km/s)	0.147	0.702	0.988	0.104	0.933
First Gravity Assist Planet	Earth	Earth	Earth	Earth	Earth
Perigee Radius 1 (km)	34570.970	32342.255	40987.783	7151.113	19785.661
Second Gravity Assist Planet	Earth	Earth	Earth	Earth	Earth
Perigee Radius 2 (km)	28356.505	87771.992	21174.207	20645.644	91586.652
LOS Angle	341.415°	54.077°	30.175°	201.362°	26.862°
Sun Angle	175.912°	168.543°	167.575°	174.940°	167.531°
Impactor Velocity (km/s)	12.271	9.541	7.213	19.394	10.213

Conclusion

Throughout this paper several possible mission types for a HAIV demonstration mission have been analyzed. The baseline HAIV architecture is the simple direct intercept missions. These types of missions have the largest number of feasible candidate target asteroids, require a minimal total post-launch ΔV (close to 0 km/s for the optimal cases presented herein), and are representative of the sort of worst case asteroid mitigation mission scenario that we should be prepared for. Table 4 shows a summary of the top 3 asteroids chosen from a search of possible target asteroids.

More advanced missions, which enable an observer spacecraft to arrive at the asteroid prior to the main spacecraft impact, have also been analyzed. The results generally show that allowing the impactor spacecraft to perform multiple gravity assists lowers the total required ΔV for each mission considered as well as increases the impactor arrival velocity. Several feasible gravity assist rendezvous missions are presented in Tables 7 and 8. There are several possible target asteroids which require a total ΔV of 1.5 km/s or less, with the lowest combined rendezvous/impact mission ΔV of approximately 600 m/s.

Appendix: Genetic Algorithm Basics

The heart of a genetic algorithm is the simulation of natural selection, reproduction, and mutations found in nature. Genetic operators are used to 'evolve' an initial population, through genetic operators, in order to determine a best fitness design [15]. The purpose of this section is to develop and implement a genetic algorithm for the MGA, MGA-DSM, and other complex mission design problems.

A genetic algorithm(GA) is a stochastic optimization method based on the principles of evolution. Genetic algorithms perform a probabilistic search by evolving a randomly chosen initial population. The population is just a series of sets of variables that are evaluated by a cost function, in this case the cost functions previously covered. The advantage of using evolutionary methods over traditional optimization methods is that no initial solution is necessary. This helps ensure, but does not guarantee, that solutions are not confined to locally optimal solutions. Genetic algorithms also perform well in very complex nonlinear design spaces. Despite all the advantages, evolutionary algorithms do have their downside. They almost always require a greater number of cost function evaluations, increasing the computational requirements. Additionally evolutionary algorithms do not make use of gradients, so there is no proof of convergence. It should also be noted that genetic algorithms were developed for constrained minimization problems and may not perform well for unconstrained minimization.

The basic genetic operators are, selection, reproduction/crossover, mutation, and elitism. The genetic algorithm developed in this section can utilize a number of different selection, reproduction, crossover, and mutation methods. Each of the methods will be discussed in detail in later sections.

In a simple genetic algorithm (SGA), each variable is represented by a binary string where individual bits are represented by 1's and 0's. This binary string is referred as a gene. The separate genes for each variable are then concatenated to form a complete chromosome. One chromosome correspond to one member of the entire population, which can number in the hundreds of thousands for some problems. This binary representation of variables means that each variable is discretized to a certain resolution. In our case the desired resolution for each variable is one of the inputs to the genetic algorithm, along with the individual variable upper and lower bounds, size of the population, and number of generations the population is to be run out. For an individual variable the resolution is defined as

$$r = \frac{x^U - x^L}{2^b - 1} \tag{45}$$

where x^U and x^L are the user specified variable upper and lower bounds, while b is the minimum number of bits required to obtain the desired variable accuracy. Eq. 45 can then be solver for b for each individual variable. With the variable b known for each variable the size of each chromosome can be determined.

Then next step in the process is to randomly, via a "digital coin flip", assign a value (1 or 0) to each position in the chromosome. The coin flip is performed using a uniform random number generator, that generates random numbers between 0 and 1. If the random number is greater than 0.5, the a value of 1 is assigned, otherwise a value of 0 is assigned. This process is run out to generate an entire initial population, which is randomly distributed throughout the design space.

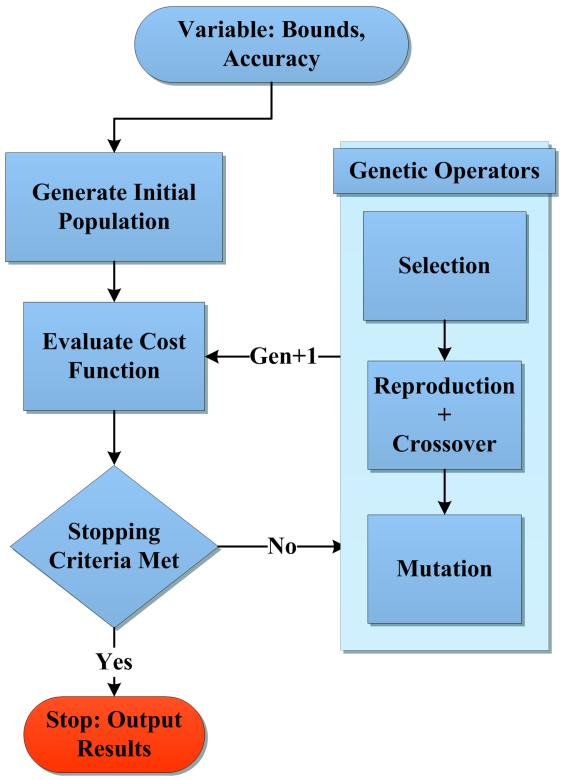

Figure 3: Simple genetic algorithm flow chart.

From this point each member of the population is assigned a fitness value, via a user supplied cost function. The genetic operators are then used to generate a new population from the initial parent population. This is the crux of how genetic algorithms are able to evolve to more fit populations. This process continues until the genetic algorithm is told to exit and output the final population. Common stopping conditions include stopping after a certain number of iterations, monitoring when the best fit solution stop changing, or monitoring when the average cost function value approaches the population minimum. For this study the stopping condition is always running the genetic algorithm out by a user specified number of generations. The sequence of operations of the core operations of the genetic algorithm is illustrated in Figure 3. One secondary operator, elitism, was used in this

genetic algorithm as well. The elitism operator ensure that the best fit solution(s) are not lost from generation to generations. A simple elitism operator is used, in which the top two solutions from the parent population are directly inserted into the next generation.

Selection Types

In genetic algorithms, selection operator, also the first genetic operator, is used to ensure that the best fit solutions are chosen to pass on their genes through the reproduction and crossover operators. The selection operator is essentially the operator that represents the survival of the fittest principle. A total of two selection types have been implemented in this genetic algorithm one based solely on a roulette selection method, and another that combines roulette and tournament selection. These two operators are by no means the only possible selection methods, but that are some of the simplest to use and prove to work well for the mission design problems.

Roulette selection is a fitness proportionate selection method in which better fit individuals are more likely to be chosen for reproduction and crossover. There are four fitness types that are used in the roulette selection method described in this section. The ultimate goal is to get a normalized fitness that ranges from 0 to 1. More fit members of the population will have a higher normalized fitness value, thus they will be more likely to be chosen for further genetic operations.

The first fitness type is the raw fitness, $r(i)$, which is the fitness values provided directly from the cost function for each population member. In this case i represents the chromosome/population number. The raw fitness is then standardized, depending on whether the problem is being minimized and maximized. If the problem is a minimization problem, the standardized fitness is the same as the raw fitness as

$$s(i) = r(i) \tag{46}$$

However, if the problem is a maximization problem, the standardized fitness becomes

$$s(i) = r_{max} - r(i) \tag{47}$$

Now the fitness is adjusted so that individual fitnesses lie between 0 and 1. The adjusted fitness is larger for better individuals. The advantage of this optional step is that small differences in the most fit individuals, those that approach an adjusted of 0, are exaggerated. This has a larger benefit when the population improves by emphasizing small differences in individuals. This effect is most exaggerated in problems where the best solution has a cost function near 0 [16, 17], as follows

$$a(i) = \frac{1}{1 + s(i)} \tag{48}$$

Now that the adjusted fitness values lie between 0 and 1 the next step is to normalize the whole population, so the sum of each normalized fitness value is 1. Ultimately, this is necessary because individuals are chosen through the use of random numbers, that also in 0 and 1 range, as

$$n(i) = \frac{a(i)}{\sum_{j}^{n} a(j)} \tag{49}$$

The actual selection of individuals, based on normalized fitness, is done in the following manner. Firstly the normalized fitnesses are sorted from largest to smallest. Next a random number is generated. This random number will decide which individual is then selected. The actual selection of an individual is done by a summation of the normalized fitness values. The individual that causes the summation value to be greater than the random number is chosen to move along through the rest of the genetic operators. This process is repeated and both of the individuals then go through the reproduction or crossover operators. Thus, more fit individuals are more likely to be passed on to the next generation.

Tournament is a greedy over selection method that also utilized the roulette selection method. Two individual are chosen using roulette selection and then compete to see which individual is allowed to pass on its genetic material. This is done through the direct comparison of their normalized fitness function. The individual with the best fitness is chosen as the one that gets to pass through to the reproduction and crossover operations. The process is repeated twice, resulting in two individuals who's genetic material can be passed on.

This selection method has a distinct advantage in that it drives down the raw fitness and average of the fitness function in fewer generations than pure roulette selection. With all greedy over selection methods there is a risk that genetic diversity, which could help out the population in later generations, will be lost. Therefore tournament selection should be used with care by the user. In the orbital problems discussed in this paper, tournament selection does appear to work well.

Reproduction and Crossover Operator Types

While the selection operator determines which population members get the privilege of reproducing and passing on their genetic material to future generations, the crossover and reproduction operators decided what to do with that genetic material. In the algorithm utilized in this paper the user must supply the probability in which an individual will under go either reproduction or crossover. These probabilities must total up to 1.0 (100%), with values typically being close to 0.9 and 0.1 for crossover and reproduction respectively. It should also noted that both operations require two parent and produce two offspring.

The simplest of these two operators is reproduction. In traditional genetic algorithm terms this means that the operation is a fitness-proportionate process in which individuals are allowed to directly pass to the next generation with a probability proportionate to their fitness values. This essentially means that when reproduction occurs the two parents are passed directly from the parent generation into the next generation. As with every other critical procedure in the genetic algorithm, whether the parents undergoes reproduction or crossover is chosen through the use of random number. In the algorithm a random number is generated. If the random number is greater than the user given crossover probability the parents undergoes reproduction. If not, the a crossover operation is applied. This, of course, is the reason that the two probabilities must total up to 100%.

The crossover process is a process in which biological reproduction is used to allow new individuals, with new and unique genetics, to be created. Unlike the reproduction process, crossovers allow new points in the design space to be searched. Without reproduction (and also mutations) genetic algorithms would be no more useful and a completely random search. The crossover operation produces to offspring from two parents that contain genetic material from both parents. A total of 4 distinct crossover types have been implemented in for use with this genetic algorithm. The user supplies which crossover type should be used, making the final genetic algorithm suitable for many different types of optimization problems. For the mission design problems discussed in this paper the double point crossover proved to be the best crossover type. However for other types of problems this may not necessarily be the cause.

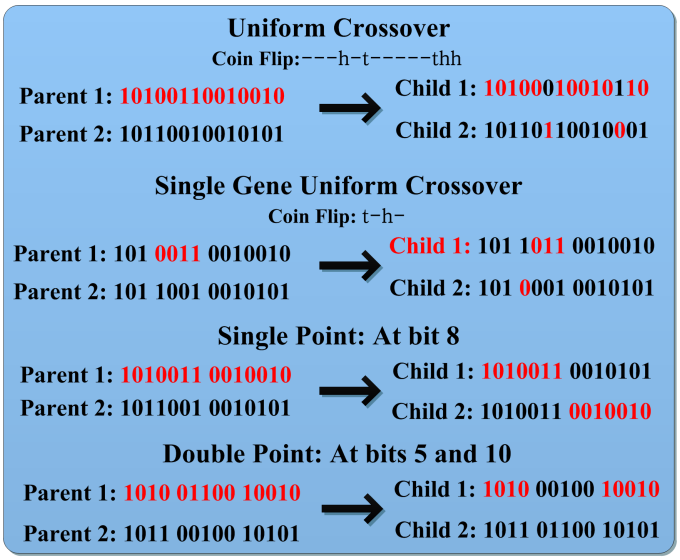

Figure 4: Simple illustration of the four implemented crossover types.

The purpose of each crossover type is to promote genetic diversity and expand, in a controlled way, the search of the design space. The first type considered is uniform crossover. It has been shown to be a very effective method for promoting genetic diversity, and in turn the discovery of new useful chromosomes [15, 18]. In uniform crossover each bit in the chromosome is a crossover point. The two offspring are generated by the same virtual coin flip that was used to initially generate the population for the first generation. If two bit are the same for both parents no coin flip is necessary. However, if two bits are not identical in the parents the coin flip is used to decide which offspring gets the genetic material from the separate parent individuals. This process is graphically shown in the first entry in Figure 4. In this case if the coin flip is heads, i.e. the random number is greater than or equal to 0.5, the bit from the second parent is inserted into the chromosome for the first child and the bit from the first

parent is inserted into the chromosome of the second child. The exact opposite is true if the coin flip is tails, i.e. the random number is less than 0.5.

A second crossover operator has also been developed that is similar to uniform crossover but only operates on an individual gene. This process only changes the value of one gene (i.e. variable). In some situations changes to an individual variable can greatly improve (or alternatively worsen) the individuals fitness. For this process a gene is randomly selected. The same gene then undergoes uniform crossover. An illustration of this method can be seen in Figure 4. In this example the second gene (bits 4-7) undergoes uniform crossover through the same virtual coin flip method described above.

In single point crossover one bit is randomly chosen to be the crossover point. All bits after the random crossover point are swapped between the two points. Double point crossover is the same thing with two randomly chosen crossover points. While these two methods are the simplest of the tested crossover methods they have proven extremely useful in practical applications.

Mutation Types

The last genetic operator, which the newly generated population must pass through, is the mutation operator. The probability that a mutation will occur and the desired type of mutation are the last two user inputs. The probability that a mutation should occur should be small, typically less than 0.05 (5%). When the mutation probability is set too high the genetic algorithm will start to resemble a simple random search. If the user doesn't wish to make use of the mutation operator, a probability of 0 can be entered as well.

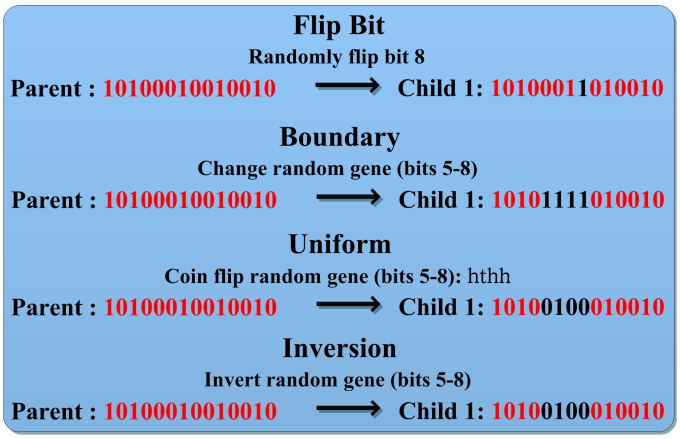

Figure 5: Simple illustration of the four mutation types implemented.

Allowing the genetic algorithm to utilize a mutation operator has several advantages. Mutations are used to help maintain genetic diversity in a population as it ages. Often times after many generations the population can lose genetic diversity and stagnate at a local minimum. Mutations help to prevent this from happening. By introducing (or in some cases reintroducing) changes in a chromosome or individual gene it is possible for better more fit individuals to appear.

As with the crossover operator four separate types of mutations have been implemented. Unlike reproduction and crossover mutations operate on a single individual in the population. Different mutation types may work well for individual problems. The four types introduced here are representative of some of the most common types of mutations used in genetic programming. Each mutation type is illustrated in Figure 5.

The simplest type of mutation is the flip bit mutation. In this type of mutation the program randomly chooses a single bit to be flipped. When a bit is flipped that value is either changed from 1 to 0 or from 0 to 1. The next three mutation types are only allowed to operate on a single randomly chosen gene.

The boundary mutation type is as simple as it sounds. An individual gene is set either to corresponding variables user supplied minimum or maximum. The digital coin flip is used to decided whether the minimum or maximum values will be used. To set the gene to the maximum every bit is set to 1. Alternative is the gene is set to the minimum every bit is changed to 0.

Uniform mutation is similar to uniform crossover and the method used to initialize the population. A digital coin flip is used to completely redefine an individual gene. The last mutation type studied, inversion, is a simple mutation operator that has proven to work extremely well for mission design problems. As the name implies, when inversion is applied the bits that make up the gene are simply inverted.

Table 9: Comparison of mutation and crossover types for a Cassini-type MGA-DSM mission or a population size of 20,000 run for 200 generations. The numbers represent the final cost function values in km/s.

Crossover Type	**Mutation Type**			
	Flip Bit	**Uniform**	**Boundary**	**Inversion**
Uniform	6.510	6.938	6.805	6.536
Uniform Gene	4.903	5.050	5.626	5.368
Single Point	5.182	4.148	4.636	4.687
Double Point	4.389	3.731	5.137	3.363

Comparison of Genetic Operator Performances

When using genetic algorithms, it is beneficial to perform a study to determine which combination or selection, crossover, and mutation operators work best with the type of problem being solved. A much more detailed study than that illustrated in Table 9 was performed when designing and implementing the genetic algorithm. None the less, Table 9 is representative of the results. In general, the best crossover type for the MGA and MGA-DSM problems is double point. It is less clear which mutation type is the best. Both the uniform and inversion operators perform well. For the following example problems, the selection, crossover, and mutation types used are tournament, double point, and inversion respectively.

Acknowledgments

This research work has been supported by a NASA Innovative Advanced Concepts (NIAC) Phase 2. The authors would like to thank Dr. John (Jay) Falker, the NIAC Program Executive, for his support.

References

[1] Morrison, D., The Spaceguard Survey: Report of the NASA International Near-Earth-Object Detection Workshop, NASA STI/Recon Technical Report N 92 (1992) 34245.

[2] Pitz, Alan and Kaplinger, Brian and Wie, Bong, Preliminary Design of a Hypervelocity Nuclear Interceptor Spacecraft for Optimal Disruption/Fragmentation of NEOs, 22nd AAS/AIAA Space Flight Mechanics Meeting AAS-12-225 (2012).

[3] Vardaxis, George and Pitz, Alan and Wie, Bong, Conceptual Design of Planetary Defense Technology Demonstration Mission, 22nd AAS/AIAA Space Flight Mechanics Meeting AAS-12-128 (2012).

[4] Winkler, Tim and Wagner, Sam and Wie, Bong, Optimal Target Selection for a Planetary Defense Technology (PDT) Demonstration Mission, 22nd AAS/AIAA Space Flight Mechanics Meeting AAS-12-226 (2012).

[5] Carnelli, Ian and G*á*lvez, Andres and Izzo, Dario, Don Quijote: A NEO Deflection Precursor Mission, 2006 NASA Near-Earth Object Detection and Threat Mitigation Workshop (2006).

[6] Cano, Juan and S*á*nchez, Mariano and Carnelli, Ian, Mission Analysis for the Don Quijote Phase-A Study, Proceedings of the 20th International Symposium on Space Flight Dynamics (2007).

[7] G*á*lvez, Andr*é*s and Carnelli, Ian, ESA's Don Quijote Mission: an Opportunity for the Investigation of an Artificial Impact Crater on an Asteroid, 25th International Symposium on Space Technology and Science (2006).

[8] Fujiwara, A. and Kawaguchi, J. and Yeomans, and All, Et., The Rubble-Pile Asteroid Itokawa as Observed by Hayabusa, Science 312 (2006) 1330–1334.

[9] Conway, Bruce, Spacecraft Trajectory Optimization, Cambridge University Press, 32 Avenue of the Americas, New York, NY 10013-2473, USA, First edition, 2010.

[10] Englander, Jacob and Conway, Bruce and Williams, Trevor, Optimal Autonomous Mission Planning Via Evolutionary Algorithms, 21th AAS/AIAA Space Flight Mechanics Meeting AAS-11-159 (2011).

[11] Vasile, Massimiliano and De Pascale, Paolo, On the Preliminary Design of Multiple Gravity-Assist Trajectories, Journal of Spacecraft and Rockets 43(4) (2009) 794–805.

[12] Wagner, Sam and Kaplinger, Brian and Wie, Bong, GPU Accelerated Genetic Algorithm for Multiple Gravity-Assist and Impulsive ΔV Maneuvers, AIAA/AAS Guidance Navigation and Control Conference AIAA 2012-4592 (2012).

[13] Wagner, Sam and Winkler, Timothy and Wie, Bong, Analysis and Selection of Optimal Targets for a Planetary Defense Technology Demonstration Mission, AIAA/AAS Guidance Navigation and Control Conference AIAA 2012-4874 (2012).

[14] Qadir, Khurram, Mult-gravity Assist Design Tool for Interplanetary Trajectory Optimisation, Master's thesis, Lulea University of Technology, 2009.

[15] Vavrina, Matthew, A Hybrid Genetic Algorithm Approach to Global Low-thrust Trajectory Optimization, Ph.D. thesis, Purdue University, 2010.

[16] Goldberg, David, Genetic Algorithms in Search, Optimization, and Machine Learning, Addison-Wesley, First edition, 1989.

[17] Koza, John, Genetic Programming: On the Programming of Computers by Means of Natural Selection, The MIT Press, Cambridge, Massachusetts, First edition, 1992.

[18] Syswerda, Gilbert, Uniform Crossover in Genetic Algorithms, in: Proceedings of the 3rd International Conference on Genetic Algorithms, Morgan Kaufmann Publishers Inc., San Francisco, CA, USA, 1989, pp. 2–.